

Measurements of the Branching Fraction and CP -Violation Asymmetries in $B^0 \rightarrow f_0(980)K_S^0$

B. Aubert,¹ R. Barate,¹ D. Boutigny,¹ F. Couderc,¹ J.-M. Gaillard,¹ A. Hicheur,¹ Y. Karyotakis,¹ J. P. Lees,¹ V. Tisserand,¹ A. Zghiche,¹ A. Palano,² A. Pompili,² J. C. Chen,³ N. D. Qi,³ G. Rong,³ P. Wang,³ Y. S. Zhu,³ G. Eigen,⁴ I. Ofte,⁴ B. Stugu,⁴ G. S. Abrams,⁵ A. W. Borgland,⁵ A. B. Breon,⁵ D. N. Brown,⁵ J. Button-Shafer,⁵ R. N. Cahn,⁵ E. Charles,⁵ C. T. Day,⁵ M. S. Gill,⁵ A. V. Gritsan,⁵ Y. Groysman,⁵ R. G. Jacobsen,⁵ R. W. Kadel,⁵ J. Kadyk,⁵ L. T. Kerth,⁵ Yu. G. Kolomensky,⁵ G. Kukartsev,⁵ G. Lynch,⁵ L. M. Mir,⁵ P. J. Oddone,⁵ T. J. Orimoto,⁵ M. Pripstein,⁵ N. A. Roe,⁵ M. T. Ronan,⁵ V. G. Shelkov,⁵ W. A. Wenzel,⁵ M. Barrett,⁶ K. E. Ford,⁶ T. J. Harrison,⁶ A. J. Hart,⁶ C. M. Hawkes,⁶ S. E. Morgan,⁶ A. T. Watson,⁶ M. Fritsch,⁷ K. Goetzen,⁷ T. Held,⁷ H. Koch,⁷ B. Lewandowski,⁷ M. Pelizaeus,⁷ M. Steinke,⁷ J. T. Boyd,⁸ N. Chevalier,⁸ W. N. Cottingham,⁸ M. P. Kelly,⁸ T. E. Latham,⁸ F. F. Wilson,⁸ T. Cuhadar-Donszelmann,⁹ C. Hearty,⁹ N. S. Knecht,⁹ T. S. Mattison,⁹ J. A. McKenna,⁹ D. Thiessen,⁹ A. Khan,¹⁰ P. Kyberd,¹⁰ L. Teodorescu,¹⁰ V. E. Blinov,¹¹ V. P. Druzhinin,¹¹ V. B. Golubev,¹¹ V. N. Ivanchenko,¹¹ E. A. Kravchenko,¹¹ A. P. Onuchin,¹¹ S. I. Serednyakov,¹¹ Yu. I. Skovpen,¹¹ E. P. Solodov,¹¹ A. N. Yushkov,¹¹ D. Best,¹² M. Bruinsma,¹² M. Chao,¹² I. Eschrich,¹² D. Kirkby,¹² A. J. Lankford,¹² M. Mandelkern,¹² R. K. Mommsen,¹² W. Roethel,¹² D. P. Stoker,¹² C. Buchanan,¹³ B. L. Hartfiel,¹³ S. D. Foulkes,¹⁴ J. W. Gary,¹⁴ B. C. Shen,¹⁴ K. Wang,¹⁴ D. del Re,¹⁵ H. K. Hadavand,¹⁵ E. J. Hill,¹⁵ D. B. MacFarlane,¹⁵ H. P. Paar,¹⁵ Sh. Rahatlou,¹⁵ V. Sharma,¹⁵ J. W. Berryhill,¹⁶ C. Campagnari,¹⁶ B. Dahmes,¹⁶ S. L. Levy,¹⁶ O. Long,¹⁶ A. Lu,¹⁶ M. A. Mazur,¹⁶ J. D. Richman,¹⁶ W. Verkerke,¹⁶ T. W. Beck,¹⁷ A. M. Eisner,¹⁷ C. A. Heusch,¹⁷ W. S. Lockman,¹⁷ T. Schalk,¹⁷ R. E. Schmitz,¹⁷ B. A. Schumm,¹⁷ A. Seiden,¹⁷ P. Spradlin,¹⁷ D. C. Williams,¹⁷ M. G. Wilson,¹⁷ J. Albert,¹⁸ E. Chen,¹⁸ G. P. Dubois-Felsmann,¹⁸ A. Dvoretzki,¹⁸ D. G. Hitlin,¹⁸ I. Narsky,¹⁸ T. Piatenko,¹⁸ F. C. Porter,¹⁸ A. Ryd,¹⁸ A. Samuel,¹⁸ S. Yang,¹⁸ S. Jayatilake,¹⁹ G. Mancinelli,¹⁹ B. T. Meadows,¹⁹ M. D. Sokoloff,¹⁹ T. Abe,²⁰ F. Blanc,²⁰ P. Bloom,²⁰ S. Chen,²⁰ W. T. Ford,²⁰ U. Nauenberg,²⁰ A. Olivas,²⁰ P. Rankin,²⁰ J. G. Smith,²⁰ J. Zhang,²⁰ L. Zhang,²⁰ A. Chen,²¹ J. L. Harton,²¹ A. Soffer,²¹ W. H. Toki,²¹ R. J. Wilson,²¹ Q. L. Zeng,²¹ D. Altenburg,²² T. Brandt,²² J. Brose,²² M. Dickopp,²² E. Feltresi,²² A. Hauke,²² H. M. Lacker,²² R. Müller-Pfefferkorn,²² R. Nogowski,²² S. Otto,²² A. Petzold,²² J. Schubert,²² K. R. Schubert,²² R. Schwierz,²² B. Spaan,²² J. E. Sundermann,²² D. Bernard,²³ G. R. Bonneaud,²³ F. Brochard,²³ P. Grenier,²³ S. Schrenk,²³ Ch. Thiebaux,²³ G. Vasileiadis,²³ M. Verderi,²³ D. J. Bard,²⁴ P. J. Clark,²⁴ D. Lavin,²⁴ F. Muheim,²⁴ S. Playfer,²⁴ Y. Xie,²⁴ M. Andreotti,²⁵ V. Azzolini,²⁵ D. Bettoni,²⁵ C. Bozzi,²⁵ R. Calabrese,²⁵ G. Cibinetto,²⁵ E. Luppi,²⁵ M. Negri,²⁵ L. Piemontese,²⁵ A. Sarti,²⁵ E. Treadwell,²⁶ R. Baldini-Ferrolli,²⁷ A. Calcaterra,²⁷ R. de Sangro,²⁷ G. Finocchiaro,²⁷ P. Patteri,²⁷ M. Piccolo,²⁷ A. Zallo,²⁷ A. Buzzo,²⁸ R. Capra,²⁸ R. Contri,²⁸ G. Crosetti,²⁸ M. Lo Vetere,²⁸ M. Macri,²⁸ M. R. Monge,²⁸ S. Passaggio,²⁸ C. Patrignani,²⁸ E. Robutti,²⁸ A. Santroni,²⁸ S. Tosi,²⁸ S. Bailey,²⁹ G. Brandenburg,²⁹ M. Morii,²⁹ E. Won,²⁹ R. S. Dubitzky,³⁰ U. Langenegger,³⁰ W. Bhimji,³¹ D. A. Bowerman,³¹ P. D. Dauncey,³¹ U. Egede,³¹ J. R. Gaillard,³¹ G. W. Morton,³¹ J. A. Nash,³¹ G. P. Taylor,³¹ M. J. Charles,³² G. J. Grenier,³² U. Mallik,³² J. Cochran,³³ H. B. Crawley,³³ J. Lamsa,³³ W. T. Meyer,³³ S. Prell,³³ E. I. Rosenberg,³³ J. Yi,³³ M. Davier,³⁴ G. Grosdidier,³⁴ A. Höcker,³⁴ S. Laplace,³⁴ F. Le Diberder,³⁴ V. Lepeltier,³⁴ A. M. Lutz,³⁴ T. C. Petersen,³⁴ S. Plaszczynski,³⁴ M. H. Schune,³⁴ L. Tantot,³⁴ G. Wormser,³⁴ C. H. Cheng,³⁵ D. J. Lange,³⁵ M. C. Simani,³⁵ D. M. Wright,³⁵ A. J. Bevan,³⁶ C. A. Chavez,³⁶ J. P. Coleman,³⁶ I. J. Forster,³⁶ J. R. Fry,³⁶ E. Gabathuler,³⁶ R. Gamet,³⁶ R. J. Parry,³⁶ D. J. Payne,³⁶ R. J. Sloane,³⁶ C. Touramanis,³⁶ J. J. Back,³⁷ C. M. Cormack,³⁷ P. F. Harrison,^{37,*} F. Di Lodovico,³⁷ G. B. Mohanty,³⁷ C. L. Brown,³⁸ G. Cowan,³⁸ R. L. Flack,³⁸ H. U. Flaecher,³⁸ M. G. Green,³⁸ P. S. Jackson,³⁸ T. R. McMahon,³⁸ S. Ricciardi,³⁸ F. Salvatore,³⁸ M. A. Winter,³⁸ D. Brown,³⁹ C. L. Davis,³⁹ J. Allison,⁴⁰ N. R. Barlow,⁴⁰ R. J. Barlow,⁴⁰ P. A. Hart,⁴⁰ M. C. Hodgkinson,⁴⁰ G. D. Lafferty,⁴⁰ A. J. Lyon,⁴⁰ J. C. Williams,⁴⁰ A. Farbin,⁴¹ W. D. Hulsbergen,⁴¹ A. Jawahery,⁴¹ D. Kovalskyi,⁴¹ C. K. Lae,⁴¹ V. Lillard,⁴¹ D. A. Roberts,⁴¹ G. Blaylock,⁴² C. Dallapiccola,⁴² K. T. Flood,⁴² S. S. Hertzbach,⁴² R. Kofler,⁴² V. B. Koptchev,⁴² T. B. Moore,⁴² S. Saremi,⁴² H. Staengle,⁴² S. Willocq,⁴² R. Cowan,⁴³ G. Sciolla,⁴³ F. Taylor,⁴³ R. K. Yamamoto,⁴³ D. J. J. Mangeol,⁴⁴ P. M. Patel,⁴⁴ S. H. Robertson,⁴⁴ A. Lazzaro,⁴⁵ F. Palombo,⁴⁵ J. M. Bauer,⁴⁶ L. Cremaldi,⁴⁶ V. Eschenburg,⁴⁶ R. Godang,⁴⁶ R. Kroeger,⁴⁶ J. Reidy,⁴⁶ D. A. Sanders,⁴⁶ D. J. Summers,⁴⁶ H. W. Zhao,⁴⁶ S. Brunet,⁴⁷ D. Côté,⁴⁷ P. Taras,⁴⁷ H. Nicholson,⁴⁸ N. Cavallo,⁴⁹ F. Fabozzi,^{49,†} C. Gatto,⁴⁹ L. Lista,⁴⁹ D. Monorchio,⁴⁹ P. Paolucci,⁴⁹ D. Piccolo,⁴⁹ C. Sciacca,⁴⁹ M. Baak,⁵⁰ H. Bulten,⁵⁰ G. Raven,⁵⁰ L. Wilden,⁵⁰ C. P. Jessop,⁵¹ J. M. LoSecco,⁵¹ T. A. Gabriel,⁵² T. Allmendinger,⁵³ B. Brau,⁵³ K. K. Gan,⁵³ K. Honscheid,⁵³ D. Hufnagel,⁵³ H. Kagan,⁵³ R. Kass,⁵³ T. Pulliam,⁵³ A. M. Rahimi,⁵³ R. Ter-Antonyan,⁵³ Q. K. Wong,⁵³ J. Brau,⁵⁴ R. Frey,⁵⁴ O. Igonkina,⁵⁴ C. T. Potter,⁵⁴ N. B. Sinev,⁵⁴ D. Strom,⁵⁴ E. Torrence,⁵⁴ F. Colecchia,⁵⁵ A. Dorigo,⁵⁵ F. Galeazzi,⁵⁵ M. Margoni,⁵⁵ M. Morandin,⁵⁵ M. Posocco,⁵⁵ M. Rotondo,⁵⁵ F. Simonetto,⁵⁵ R. Stroili,⁵⁵ G. Tiozzo,⁵⁵ C. Voci,⁵⁵ M. Benayoun,⁵⁶ H. Briand,⁵⁶ J. Chauveau,⁵⁶ P. David,⁵⁶ Ch. de la Vaissière,⁵⁶ L. Del Buono,⁵⁶

O. Hamon,⁵⁶ M. J. J. John,⁵⁶ Ph. Leruste,⁵⁶ J. Malcles,⁵⁶ J. Ocariz,⁵⁶ M. Pivk,⁵⁶ L. Roos,⁵⁶ S. T'Jampens,⁵⁶ G. Therin,⁵⁶ P. F. Manfredi,⁵⁷ V. Re,⁵⁷ P. K. Behera,⁵⁸ L. Gladney,⁵⁸ Q. H. Guo,⁵⁸ J. Panetta,⁵⁸ F. Anulli,^{27,59} M. Biasini,⁵⁹ I. M. Peruzzi,^{27,59} M. Pioppi,⁵⁹ C. Angelini,⁶⁰ G. Batignani,⁶⁰ S. Bettarini,⁶⁰ M. Bondioli,⁶⁰ F. Bucci,⁶⁰ G. Calderini,⁶⁰ M. Carpinelli,⁶⁰ V. Del Gamba,⁶⁰ F. Forti,⁶⁰ M. A. Giorgi,⁶⁰ A. Lusiani,⁶⁰ G. Marchiori,⁶⁰ F. Martinez-Vidal,^{60,‡} M. Morganti,⁶⁰ N. Neri,⁶⁰ E. Paoloni,⁶⁰ M. Rama,⁶⁰ G. Rizzo,⁶⁰ F. Sandrelli,⁶⁰ J. Walsh,⁶⁰ M. Haire,⁶¹ D. Judd,⁶¹ K. Paick,⁶¹ D. E. Wagoner,⁶¹ N. Danielson,⁶² P. Elmer,⁶² Y. P. Lau,⁶² C. Lu,⁶² V. Miftakov,⁶² J. Olsen,⁶² A. J. S. Smith,⁶² A. V. Telnov,⁶² F. Bellini,⁶³ G. Cavoto,^{62,63} R. Faccini,⁶³ F. Ferrarotto,⁶³ F. Ferroni,⁶³ M. Gaspero,⁶³ L. Li Gioi,⁶³ M. A. Mazzoni,⁶³ S. Morganti,⁶³ M. Pierini,⁶³ G. Piredda,⁶³ F. Safai Tehrani,⁶³ C. Voena,⁶³ S. Christ,⁶⁴ G. Wagner,⁶⁴ R. Waldi,⁶⁴ T. Adye,⁶⁵ N. De Groot,⁶⁵ B. Franek,⁶⁵ N. I. Geddes,⁶⁵ G. P. Gopal,⁶⁵ E. O. Olaiya,⁶⁵ R. Aleksan,⁶⁶ S. Emery,⁶⁶ A. Gaidot,⁶⁶ S. F. Ganzhur,⁶⁶ P.-F. Giraud,⁶⁶ G. Hamel de Monchenault,⁶⁶ W. Kozanecki,⁶⁶ M. Langer,⁶⁶ M. Legendre,⁶⁶ G. W. London,⁶⁶ B. Mayer,⁶⁶ G. Schott,⁶⁶ G. Vasseur,⁶⁶ Ch. Yèche,⁶⁶ M. Zito,⁶⁶ M. V. Purohit,⁶⁷ A. W. Weidemann,⁶⁷ J. R. Wilson,⁶⁷ F. X. Yumiceva,⁶⁷ D. Aston,⁶⁸ R. Bartoldus,⁶⁸ N. Berger,⁶⁸ A. M. Boyarski,⁶⁸ O. L. Buchmueller,⁶⁸ M. R. Convery,⁶⁸ M. Cristinziani,⁶⁸ G. De Nardo,⁶⁸ D. Dong,⁶⁸ J. Dorfan,⁶⁸ D. Dujmic,⁶⁸ W. Dunwoodie,⁶⁸ E. E. Elsen,⁶⁸ S. Fan,⁶⁸ R. C. Field,⁶⁸ T. Glanzman,⁶⁸ S. J. Gowdy,⁶⁸ T. Hadig,⁶⁸ V. Halyo,⁶⁸ C. Hast,⁶⁸ T. Hryn'ova,⁶⁸ W. R. Innes,⁶⁸ M. H. Kelsey,⁶⁸ P. Kim,⁶⁸ M. L. Kocian,⁶⁸ D. W. G. S. Leith,⁶⁸ J. Libby,⁶⁸ S. Luitz,⁶⁸ V. Luth,⁶⁸ H. L. Lynch,⁶⁸ H. Marsiske,⁶⁸ R. Messner,⁶⁸ D. R. Muller,⁶⁸ C. P. O'Grady,⁶⁸ V. E. Ozcan,⁶⁸ A. Perazzo,⁶⁸ M. Perl,⁶⁸ S. Petrak,⁶⁸ B. N. Ratcliff,⁶⁸ A. Roodman,⁶⁸ A. A. Salnikov,⁶⁸ R. H. Schindler,⁶⁸ J. Schwiening,⁶⁸ G. Simi,⁶⁸ A. Snyder,⁶⁸ A. Soha,⁶⁸ J. Stelzer,⁶⁸ D. Su,⁶⁸ M. K. Sullivan,⁶⁸ J. Va'vra,⁶⁸ S. R. Wagner,⁶⁸ M. Weaver,⁶⁸ A. J. R. Weinstein,⁶⁸ W. J. Wisniewski,⁶⁸ M. Wittgen,⁶⁸ D. H. Wright,⁶⁸ A. K. Yarritu,⁶⁸ C. C. Young,⁶⁸ P. R. Burchat,⁶⁹ A. J. Edwards,⁶⁹ T. I. Meyer,⁶⁹ B. A. Petersen,⁶⁹ C. Roat,⁶⁹ S. Ahmed,⁷⁰ M. S. Alam,⁷⁰ J. A. Ernst,⁷⁰ M. A. Saeed,⁷⁰ M. Saleem,⁷⁰ F. R. Wappler,⁷⁰ W. Bugg,⁷¹ M. Krishnamurthy,⁷¹ S. M. Spanier,⁷¹ R. Eckmann,⁷² H. Kim,⁷² J. L. Ritchie,⁷² A. Satpathy,⁷² R. F. Schwitters,⁷² J. M. Izen,⁷³ I. Kitayama,⁷³ X. C. Lou,⁷³ S. Ye,⁷³ F. Bianchi,⁷⁴ M. Bona,⁷⁴ F. Gallo,⁷⁴ D. Gamba,⁷⁴ C. Borean,⁷⁵ L. Bosisio,⁷⁵ C. Cartaro,⁷⁵ F. Cossutti,⁷⁵ G. Della Ricca,⁷⁵ S. Dittongo,⁷⁵ S. Grancagnolo,⁷⁵ L. Lanceri,⁷⁵ P. Poropat,^{75,8} L. Vitale,⁷⁵ G. Vuagnin,⁷⁵ R. S. Panvini,⁷⁶ Sw. Banerjee,⁷⁷ C. M. Brown,⁷⁷ D. Fortin,⁷⁷ P. D. Jackson,⁷⁷ R. Kowalewski,⁷⁷ J. M. Roney,⁷⁷ H. R. Band,⁷⁸ S. Dasu,⁷⁸ M. Datta,⁷⁸ A. M. Eichenbaum,⁷⁸ M. Graham,⁷⁸ J. J. Hollar,⁷⁸ J. R. Johnson,⁷⁸ P. E. Kutter,⁷⁸ H. Li,⁷⁸ R. Liu,⁷⁸ A. Mihalys,⁷⁸ A. K. Mohapatra,⁷⁸ Y. Pan,⁷⁸ R. Prepost,⁷⁸ A. E. Rubin,⁷⁸ S. J. Sekula,⁷⁸ P. Tan,⁷⁸ J. H. von Wimmersperg-Toeller,⁷⁸ J. Wu,⁷⁸ S. L. Wu,⁷⁸ Z. Yu,⁷⁸ M. G. Greene,⁷⁹ and H. Neal⁷⁹

(BABAR Collaboration)

¹Laboratoire de Physique des Particules, F-74941 Annecy-le-Vieux, France

²Dipartimento di Fisica and INFN, Università di Bari, I-70126 Bari, Italy

³Institute of High Energy Physics, Beijing 100039, China

⁴University of Bergen, Institute of Physics, N-5007 Bergen, Norway

⁵Lawrence Berkeley National Laboratory and University of California, Berkeley, California 94720, USA

⁶University of Birmingham, Birmingham, B15 2TT, United Kingdom

⁷Institut für Experimentalphysik I, Ruhr Universität Bochum, D-44780 Bochum, Germany

⁸University of Bristol, Bristol BS8 1TL, United Kingdom

⁹University of British Columbia, Vancouver, British Columbia, Canada V6T 1Z1

¹⁰Brunel University, Uxbridge, Middlesex UB8 3PH, United Kingdom

¹¹Budker Institute of Nuclear Physics, Novosibirsk 630090, Russia

¹²University of California at Irvine, Irvine, California 92697, USA

¹³University of California at Los Angeles, Los Angeles, California 90024, USA

¹⁴University of California at Riverside, Riverside, California 92521, USA

¹⁵University of California at San Diego, La Jolla, California 92093, USA

¹⁶University of California at Santa Barbara, Santa Barbara, California 93106, USA

¹⁷Institute for Particle Physics, University of California at Santa Cruz, Santa Cruz, California 95064, USA

¹⁸California Institute of Technology, Pasadena, California 91125, USA

¹⁹University of Cincinnati, Cincinnati, Ohio 45221, USA

²⁰University of Colorado, Boulder, Colorado 80309, USA

²¹Colorado State University, Fort Collins, Colorado 80523, USA

²²Institut für Kern- und Teilchenphysik, Technische Universität Dresden, D-01062 Dresden, Germany

²³Ecole Polytechnique, LLR, F-91128 Palaiseau, France

²⁴University of Edinburgh, Edinburgh EH9 3JZ, United Kingdom

²⁵Dipartimento di Fisica and INFN, Università di Ferrara, I-44100 Ferrara, Italy

- ²⁶Florida A&M University, Tallahassee, Florida 32307, USA
²⁷Laboratori Nazionali di Frascati dell'INFN, I-00044 Frascati, Italy
²⁸Dipartimento di Fisica and INFN, Università di Genova, I-16146 Genova, Italy
²⁹Harvard University, Cambridge, Massachusetts 02138, USA
³⁰Physikalisches Institut, Universität Heidelberg, Philosophenweg 12, D-69120 Heidelberg, Germany
³¹Imperial College London, London, SW7 2AZ, United Kingdom
³²University of Iowa, Iowa City, Iowa 52242, USA
³³Iowa State University, Ames, Iowa 50011-3160, USA
³⁴Laboratoire de l'Accélérateur Linéaire, F-91898 Orsay, France
³⁵Lawrence Livermore National Laboratory, Livermore, California 94550, USA
³⁶University of Liverpool, Liverpool L69 7ZE, United Kingdom
³⁷Queen Mary, University of London, E1 4NS, United Kingdom
³⁸Royal Holloway and Bedford New College, University of London, Egham, Surrey TW20 0EX, United Kingdom
³⁹University of Louisville, Louisville, Kentucky 40292, USA
⁴⁰University of Manchester, Manchester M13 9PL, United Kingdom
⁴¹University of Maryland, College Park, Maryland 20742, USA
⁴²University of Massachusetts, Amherst, Massachusetts 01003, USA
⁴³Laboratory for Nuclear Science, Massachusetts Institute of Technology, Cambridge, Massachusetts 02139, USA
⁴⁴McGill University, Montréal, Quebec, Canada H3A 2T8
⁴⁵Dipartimento di Fisica and INFN, Università di Milano, I-20133 Milano, Italy
⁴⁶University of Mississippi, University, Mississippi 38677, USA
⁴⁷Laboratoire René J. A. Lévesque, Université de Montréal, Montréal, Quebec, Canada H3C 3J7
⁴⁸Mount Holyoke College, South Hadley, Massachusetts 01075, USA
⁴⁹Dipartimento di Scienze Fisiche and INFN, Università di Napoli Federico II, I-80126, Napoli, Italy
⁵⁰NIKHEF, National Institute for Nuclear Physics and High Energy Physics, NL-1009 DB Amsterdam, The Netherlands
⁵¹University of Notre Dame, Notre Dame, Indiana 46556, USA
⁵²Oak Ridge National Laboratory, Oak Ridge, Tennessee 37831, USA
⁵³Ohio State University, Columbus, Ohio 43210, USA
⁵⁴University of Oregon, Eugene, Oregon 97403, USA
⁵⁵Dipartimento di Fisica and INFN, Università di Padova, I-35131 Padova, Italy
⁵⁶Laboratoire de Physique Nucléaire et de Hautes Energies, Universités Paris VI et VII, F-75252 Paris, France
⁵⁷Dipartimento di Elettronica and INFN, Università di Pavia, I-27100 Pavia, Italy
⁵⁸University of Pennsylvania, Philadelphia, Pennsylvania 19104, USA
⁵⁹Dipartimento di Fisica and INFN, Università di Perugia, I-06100 Perugia, Italy
⁶⁰Dipartimento di Fisica, Scuola Normale Superiore and INFN, Università di Pisa, I-56127 Pisa, Italy
⁶¹Prairie View A&M University, Prairie View, Texas 77446, USA
⁶²Princeton University, Princeton, New Jersey 08544, USA
⁶³Dipartimento di Fisica and INFN, Università di Roma La Sapienza, I-00185 Roma, Italy
⁶⁴Universität Rostock, D-18051 Rostock, Germany
⁶⁵Rutherford Appleton Laboratory, Chilton, Didcot, Oxon OX11 0QX, United Kingdom
⁶⁶DSM/Dapnia, CEA/Saclay, F-91191 Gif-sur-Yvette, France
⁶⁷University of South Carolina, Columbia, South Carolina 29208, USA
⁶⁸Stanford Linear Accelerator Center, Stanford, California 94309, USA
⁶⁹Stanford University, Stanford, California 94305-4060, USA
⁷⁰State University of New York, Albany, New York 12222, USA
⁷¹University of Tennessee, Knoxville, Tennessee 37996, USA
⁷²University of Texas at Austin, Austin, Texas 78712, USA
⁷³University of Texas at Dallas, Richardson, Texas 75083, USA
⁷⁴Dipartimento di Fisica Sperimentale and INFN, Università di Torino, I-10125 Torino, Italy
⁷⁵Dipartimento di Fisica and INFN, Università di Trieste, I-34127 Trieste, Italy
⁷⁶Vanderbilt University, Nashville, Tennessee 37235, USA
⁷⁷University of Victoria, Victoria, BC, Canada V8W 3P6
⁷⁸University of Wisconsin, Madison, Wisconsin 53706, USA
⁷⁹Yale University, New Haven, Connecticut 06511, USA

(Received 15 June 2004; published 2 February 2005)

We present measurements of the branching fraction and CP -violating asymmetries in the decay $B^0 \rightarrow f_0(980)K_S^0$. The results are obtained from a data sample of $123 \times 10^6 Y(4S) \rightarrow B\bar{B}$ decays. From a time-dependent maximum likelihood fit, we measure the branching fraction $\mathcal{B}(B^0 \rightarrow f_0(980)(\rightarrow \pi^+ \pi^-)K^0) = (6.0 \pm 0.9 \pm 0.6 \pm 1.2) \times 10^{-6}$, the mixing-induced CP violation parameter $S = -1.62_{-0.51}^{+0.56} \pm 0.09 \pm 0.04$, and the direct CP violation parameter $C = 0.27 \pm 0.36 \pm 0.10 \pm 0.07$, where the first errors are

statistical, the second systematic, and the third due to model uncertainties. We measure the $f_0(980)$ mass and width to be $m_{f_0}(980) = (980.6 \pm 4.1 \pm 0.5 \pm 4.0) \text{ MeV}/c^2$ and $\Gamma_{f_0}(980) = (43_{-9}^{+12} \pm 3 \pm 9) \text{ MeV}/c^2$, respectively.

DOI: 10.1103/PhysRevLett.94.041802

PACS numbers: 13.25.Hw, 11.30.Er, 12.15.Hh

In the standard model (SM), CP violation arises from a single phase in the three-generation Cabibbo-Kobayashi-Maskawa (CKM) quark-mixing matrix [1]. Possible indications of physics beyond the SM may be observed in the time-dependent CP asymmetries of B decays dominated by penguin-type diagrams to states such as ϕK^0 , $\eta' K^0$, $K^+ K^- K^0$, and $f_0(980) K^0$ [2]. Neglecting CKM-suppressed amplitudes, these decays carry the same weak phase as the decay $B^0 \rightarrow J/\psi K^0$ [3]. As a consequence, their mixing-induced CP -violation parameter is expected to be $-\eta_f \times \sin 2\beta = -\eta_f \times 0.74 \pm 0.05$ [4] in the SM, where η_f is the CP eigenvalue of the final state f , which is $+1$ for $f_0(980) K_S^0$. There is no direct CP violation expected in these decays since they are dominated by a single amplitude in the SM. Because of the large virtual mass scales occurring in the penguin loops, additional diagrams with non-SM heavy particles in the loops and new CP -violating phases may contribute. Measurements of CP violation in these channels and their comparisons with the SM expectation are therefore sensitive probes for physics beyond the SM. The modes ϕK^0 , $K^+ K^- K_S^0$, and $\eta' K_S^0$ have been measured by both the *BABAR* [5] and Belle experiments. Interest in s -penguin modes has intensified since the Belle collaboration measured $\sin 2\beta = -0.96 \pm 0.50_{-0.11}^{+0.09}$ in the decay $B^0 \rightarrow \phi K_S^0$, while the *BABAR* collaboration (with a sample of approximately 114 million $B\bar{B}$ pairs) measured $\sin 2\beta = 0.47 \pm 0.34(\text{stat})_{-0.06}^{+0.08}(\text{syst})$ in the decay $B^0 \rightarrow \phi K^0$.

In this Letter we present the first measurement of the branching fraction and CP -violating asymmetries in the penguin-dominated decay $B^0 \rightarrow f_0 K_S^0$ [7] from a time-dependent maximum likelihood analysis. We also measure the mass and width of the f_0 resonance. We restrict the analysis to the region of the $\pi^+ \pi^- K_S^0$ Dalitz plot that is dominated by the f_0 and we refer to this as the quasi-two-body (Q2B) approach. Effects due to the interference between the f_0 and the other resonances in the Dalitz plot are taken as systematic uncertainties.

The data we use in this analysis were accumulated with the *BABAR* detector [8] at the PEP-II asymmetric-energy $e^+ e^-$ storage ring at SLAC. The data sample consists of an integrated luminosity of 111.2 fb^{-1} collected at the $Y(4S)$ resonance (“on-resonance”) corresponding to $(122.6 \pm 0.7) \times 10^6$ $B\bar{B}$ pairs, and 11.8 fb^{-1} collected about 40 MeV below the $Y(4S)$ (“off-resonance”). In Ref. [8] we describe the silicon vertex tracker and drift chamber used for track and vertex reconstruction, and the Čerenkov detector (DIRC), the electromagnetic calorimeter (EMC), and the instrumented flux return (IFR) used for particle identification.

If we denote by Δt the difference between the proper times of the decay of the fully reconstructed $B^0 \rightarrow f_0 K_S^0$ (B_{rec}^0) and the decay of the other meson (B_{tag}^0), the time-dependent decay rate $f_{Q_{\text{tag}}}$ is given by

$$f_{Q_{\text{tag}}}(\Delta t) = \frac{e^{-|\Delta t|/\tau}}{4\tau} [1 + Q_{\text{tag}} S \sin(\Delta m_d \Delta t) - Q_{\text{tag}} C \cos(\Delta m_d \Delta t)], \quad (1)$$

where $Q_{\text{tag}} = 1(-1)$ when the tagging meson B_{tag}^0 is a $B^0(\bar{B}^0)$, τ is the mean B^0 lifetime, and Δm_d is the $B^0 \bar{B}^0$ oscillation frequency corresponding to the mass difference. The parameter S is nonzero if there is mixing-induced CP violation while a nonzero value for C would indicate direct CP violation.

We reconstruct $B^0 \rightarrow f_0(\rightarrow \pi^+ \pi^-) K_S^0$ candidates from combinations of two tracks and a K_S^0 decaying to $\pi^+ \pi^-$. For the $\pi^+ \pi^-$ pair from the f_0 candidate, we use information from the tracking system, EMC, and DIRC to remove tracks consistent with electron, kaon, or proton hypotheses. In addition, we require at least one track to have a signature in the IFR that is inconsistent with the muon hypothesis. The mass of the f_0 candidate must satisfy $0.86 < m(\pi^+ \pi^-) < 1.10 \text{ GeV}/c^2$. To reduce combinatorial background from low energy pions, we require $|\cos\theta(\pi^+)| < 0.9$, where $\theta(\pi^+)$ is the angle between the positive pion in the f_0 rest frame and the f_0 flight direction in the laboratory frame. The K_S^0 candidate is required to have a mass within $10 \text{ MeV}/c^2$ of the nominal K^0 mass [4] and a decay vertex separated from the B^0 decay vertex by at least 5 standard deviations. In addition, the cosine of the angle between the K_S^0 flight direction and the vector between the f_0 and the K_S^0 vertices must be greater than 0.99.

Two kinematic variables are used to discriminate between signal- B decays and combinatorial background. One variable is the difference ΔE between the measured center-of-mass (c.m.) energy of the B candidate and $\sqrt{s}/2$, where \sqrt{s} is the c.m. energy. The other variable is the beam-energy-substituted mass $m_{\text{ES}} \equiv \sqrt{(s/2 + \mathbf{p}_i \cdot \mathbf{p}_B)^2/E_i^2 - \mathbf{p}_B^2}$, where the B momentum \mathbf{p}_B and the four-momentum of the initial state (E_i, \mathbf{p}_i) are defined in the laboratory frame. We require $5.23 < m_{\text{ES}} < 5.29 \text{ GeV}/c^2$ and $|\Delta E| < 0.1 \text{ GeV}$.

Continuum $e^+ e^- \rightarrow q\bar{q}$ ($q = u, d, s, c$) events are the dominant background. To enhance discrimination between signal and continuum, we use a neural network (NN) to combine four variables: the cosine of the angle between the B_{rec}^0 direction and the beam axis in the c.m., the cosine of the angle between the thrust axis of the B_{rec}^0 candidate and the beam axis, and the zeroth and second angular moments

$L_{0,2}$ of the energy flow about the B_{rec}^0 thrust axis. The moments are defined by $L_j = \sum_i p_i \times |\cos\theta_i|^j$, where θ_i is the angle with respect to the B_{rec}^0 thrust axis of the track or neutral cluster i and p_i is its momentum. The sum excludes the B_{rec}^0 candidate. The NN is trained with off-resonance data and simulated signal events. The final sample of signal candidates is selected with a cut on the NN output that retains $\sim 97\%$ (52%) of the signal (continuum).

The signal efficiency determined from Monte Carlo (MC) simulation is $(37.2 \pm 3.1)\%$. MC simulation shows that 4.7% of the selected signal events are misreconstructed, mostly due to combinatorial background from low-momentum tracks used to form the f_0 candidate. In total, 7556 on-resonance events pass all selection criteria.

We use MC-simulated events to study the background from other B decays. The charmless decay modes are grouped into eight classes with similar kinematic and topological properties. The modes that decay to the $\pi^+\pi^-K_S^0$ final state are of particular importance since they have signal-like ΔE and m_{ES} distributions and their decay amplitudes interfere with the $f_0K_S^0$ decay amplitude. Among these modes are $\rho^0K_S^0$, $f_0(1370)K_S^0$, $f_2(1270)K_S^0$, $K^{*+}\pi^-$ (including other kaon resonances decaying to $K_S^0\pi^+$), and nonresonant $\pi^+\pi^-K_S^0$ decays. The inclusive charmless $\pi^+\pi^-K_S^0$ branching fraction $(23.4 \pm 3.3) \times 10^{-6}$ [9], together with the available exclusive measurements [9,10], are used to infer upper limits on the branching fractions of these decays. Along with selection efficiencies obtained from MC, these branching fractions are used to estimate the expected background. The charmed decays $B^0 \rightarrow D^-\pi^+ \rightarrow K_S^0\pi^-\pi^+$ and $B^+ \rightarrow \bar{D}^0\pi^+ \rightarrow K_S^0\pi^0\pi^+$ contribute significantly to the selected data sample. Each of these modes is treated as a separate class. Two additional classes account for the remaining neutral and charged $b \rightarrow c$ decays. In the selected data sample, we expect 45 ± 15 charmless and 128 ± 74 $b \rightarrow c$ events.

The time difference Δt is obtained from the measured distance between the z positions (along the beam direction) of the B_{rec}^0 and B_{tag}^0 decay vertices, and the boost $\beta\gamma = 0.56$ of the e^+e^- system [11,12]. To determine the flavor of the B_{tag}^0 , we use the tagging algorithm of Ref. [12]. This produces four mutually exclusive tagging categories. We also retain untagged events in a fifth category to improve the efficiency of the signal selection.

We use an unbinned maximum likelihood fit to extract the $f_0K_S^0$ event yield, the CP parameters defined in Eq. (1), and the f_0 resonance parameters. The likelihood function for the N_k candidates tagged in category k is

$$\mathcal{L}_k = e^{-N'_k} \prod_{i=1}^{N_k} \left\{ N_S \epsilon_k \mathcal{P}_{i,k}^S + N_{C,k} \mathcal{P}_{i,k}^C + \sum_{j=1}^{N_B} N_{B,j} \epsilon_{j,k} \mathcal{P}_{i,j,k}^B \right\}, \quad (2)$$

where N'_k is the sum of the signal, continuum, and the N_B B

background yields tagged in category k , N_S is the number of $f_0K_S^0$ signal events in the sample, ϵ_k is the fraction of signal events tagged in category k , $N_{C,k}$ is the number of continuum-background events that are tagged in category k , and $N_{B,j} \epsilon_{j,k}$ is the number of B -background events of class j that are tagged in category k . The B -background event yields are fixed parameters, with the exception of the $D^-\pi^+$ yield. Since $B^0 \rightarrow D^-\pi^+$ events have a characteristic distribution in $\cos\theta(\pi^+)$, well separated from continuum and $f_0K_S^0$ events, the $D^-\pi^+$ is free to vary in the fit along with the signal and continuum yields. The total likelihood \mathcal{L} is the product of the likelihoods for each tagging category.

The probability density functions (PDFs) \mathcal{P}_k^S , \mathcal{P}_k^C , and $\mathcal{P}_{j,k}^B$, for signal, continuum-background, and B -background class j , respectively, are the products of the PDFs of six discriminating variables. The signal PDF is thus given by $\mathcal{P}_k^S = \mathcal{P}^S(m_{\text{ES}}) \cdot \mathcal{P}^S(\Delta E) \cdot \mathcal{P}_k^S(\text{NN}) \cdot \mathcal{P}^S(|\cos\theta(\pi^+)|) \cdot \mathcal{P}^S(m(\pi^+\pi^-)) \cdot \mathcal{P}_k^S(\Delta t)$, where $\mathcal{P}_k^S(\Delta t)$ contains the time-dependent CP parameters defined in Eq. (1), diluted by the effects of mistagging and the Δt resolution.

The signal PDFs are decomposed into distinct distributions for correctly reconstructed and misreconstructed signal events. The fractions of misreconstructed signal events per tagging category are estimated by MC simulation. The m_{ES} , ΔE , NN, $|\cos\theta(\pi^+)|$, and $m(\pi^+\pi^-)$ PDFs for signal and B background are taken from the simulation except for the means of the signal Gaussian PDFs for m_{ES} and ΔE , and the mass and width of the f_0 , which are free to vary in the fit. We use a relativistic Breit-Wigner function to parametrize the f_0 resonance. The Δt -resolution function for signal and B -background events is a sum of three Gaussian distributions, with parameters determined by a fit to fully reconstructed B^0 decays [12]. The continuum Δt distribution is parametrized as the sum of three Gaussian distributions with two distinct means and three distinct widths, which are scaled by the Δt per-event error. For the B -background modes that are CP eigenstates, the parameters C and S are fixed to 0 and $\pm \sin 2\beta$, respectively, depending on their CP eigenvalues. For continuum, four tag asymmetries and the five yields $N_{C,k}$ are free. The signal yield, S , C , and the f_0 mass and width are among the 41 parameters that are free to vary in the fit. The majority of the free parameters are used to describe the shape of the continuum background.

The contributions to the systematic error on the signal parameters are summarized in Table I. To estimate the errors due to the fit procedure, we perform fits on a large number of MC samples with the proportions of signal, continuum, and B -background events measured from data. Biases of a few percent observed in these fits are due to imperfections in the likelihood model such as neglected correlations between the discriminating variables

TABLE I. Summary of systematic uncertainties. The uncertainties on m_{f_0} and Γ_{f_0} are in units of MeV/c^2 .

Error source	S	C	$\mathcal{B} \times 10^{-6}$	m_{f_0}	Γ_{f_0}
Fitting procedure	0.06	0.07	0.26	0.5	1.0
B background	0.05	0.05	0.30	0.2	3.0
Δt model	0.03	0.02	0.03	0.0	0.1
Tagging fraction	0.04	0.02	0.01	0.0	0.2
Signal model	0.02	0.01	0.03	0.1	0.2
DCS decays	0.01	0.04	0.00	0.0	0.0
Δm_d and τ	0.01	0.00	0.01	0.0	0.1
Tracking and PID	0.00	0.00	0.49	0.0	0.0
Subtotal	0.09	0.10	0.63	0.5	3.2
Q2B approximation	0.04	0.07	1.21	4.0	8.5

of the signal and B -background PDFs and are assigned as a systematic uncertainty of the fit procedure. The error due to the fit procedure includes the statistical error on the bias added in quadrature with the observed bias. The expected event yields from the B -background modes are varied according to the uncertainties in the measured or estimated branching fractions. Since B -background modes may exhibit CP violation, the corresponding parameters are varied within their physical ranges. We vary the parameters of the Δt model and tagging fractions incoherently within their

errors and assign as a systematic error the quadratic sum of the observed changes in our measured parameters. The uncertainties due to the simulated signal PDFs are obtained from a control sample of fully reconstructed $B^0 \rightarrow D^-(\rightarrow K_S^0 \pi^-) \pi^+$ decays. The systematic errors due to interference between the doubly Cabibbo-suppressed (DCS) $\bar{b} \rightarrow \bar{u} c \bar{d}$ amplitude with the Cabibbo-favored $\bar{b} \rightarrow \bar{c} u \bar{d}$ amplitude for tag-side B decays have been estimated from simulation by varying freely all relevant strong phases [13]. The errors associated with Δm_d and τ are estimated by varying these parameters within the errors on the world average [4].

The systematic error introduced in the Q2B approximation by ignoring interference effects between the f_0 and the other resonances in the Dalitz plot (as listed earlier) is estimated from simulation by varying freely all relative strong phases and taking the largest observed change in each parameter as the error. While the systematic errors due to interference are comparable to the statistical error for the branching fraction and the f_0 mass and width, they are small compared to the statistical error for S and C .

The maximum likelihood fit results in the $f_0 K_S^0$ event yield $N_S = 93.6 \pm 13.6 \pm 6.3$, where the first error is statistical and the second systematic. The branching fraction corresponding to this yield is

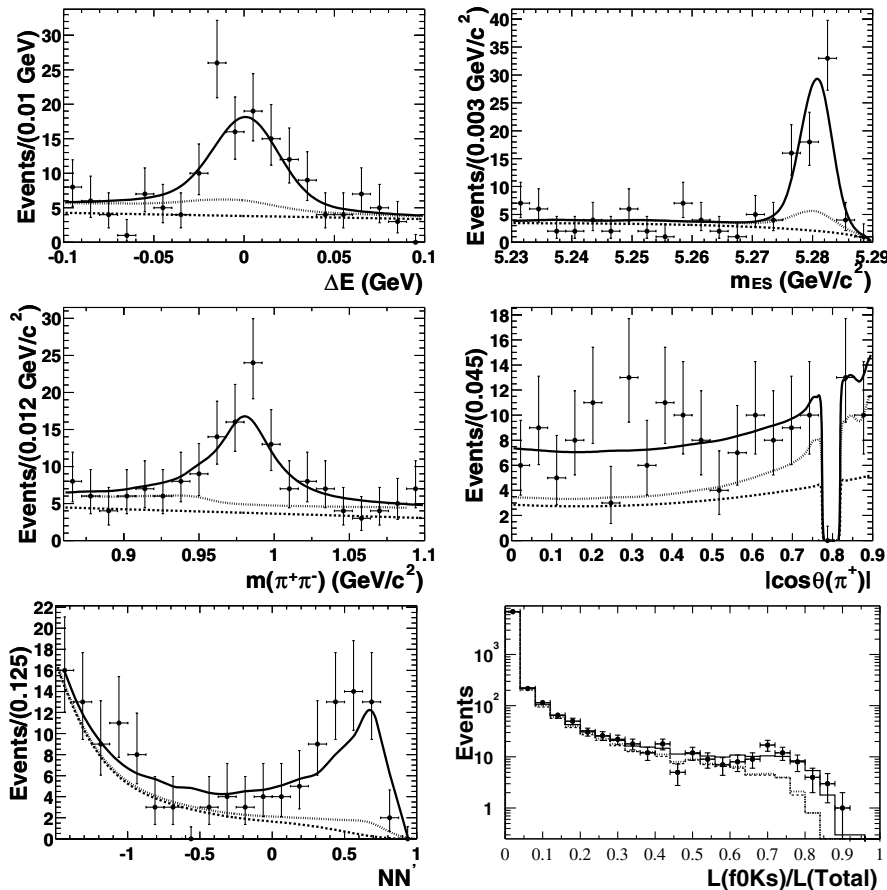


FIG. 1. Distributions of (clockwise from bottom left) NN , $m(\pi^+\pi^-)$, ΔE , m_{ES} , and $|\cos\theta(\pi^+)|$ for samples enhanced in the $f_0 K_S^0$ signal. For presentation purposes, the region $0.765 < |\cos\theta(\pi^+)| < 0.81$ has been removed to suppress the contribution from $D^-\pi^+$ events. The bottom-right plot shows the distribution of the ratio of the signal likelihood to the total likelihood for all events entering the fit. In each plot, the solid curve represents a projection of the maximum likelihood fit result, the dashed curve represents the contribution from continuum events, and the dotted line indicates the combined contributions from continuum and B -background events.

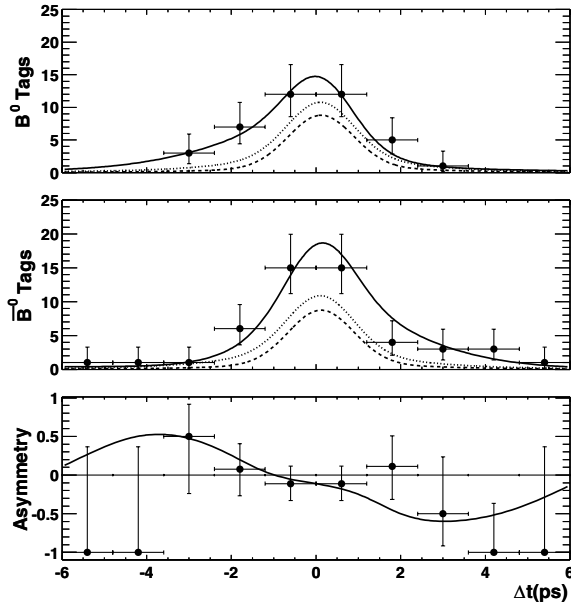


FIG. 2. The signal-enhanced time distributions tagged as B^0_{tag} (top) and \bar{B}^0_{tag} (middle), and the asymmetry, A_{B^0/\bar{B}^0} (bottom). The solid curve is a projection of the fit result. The dashed line is the distribution for continuum background and the dotted line is the total B - and continuum-background contribution.

$$\begin{aligned} \mathcal{B}(B^0 \rightarrow f_0(980)K^0) \times \mathcal{B}(f_0(980) \rightarrow \pi^+ \pi^-) \\ = (6.0 \pm 0.9 \pm 0.6 \pm 1.2) \times 10^{-6}, \end{aligned}$$

where the first error is statistical, the second systematic, and the third accounts for the model dependence in the quasi-two-body approximation. The systematic error includes an uncertainty of 8.2% from differences between data and MC in tracking, particle identification (PID), and K_S^0 detection efficiencies. Figure 1 shows distributions of ΔE , m_{ES} , $|\cos\theta(\pi^+)|$, $m(\pi^+ \pi^-)$, and NN that are enhanced in signal content by cuts on the signal-to-continuum likelihood ratios of the other discriminating variables for both data and the likelihood model after fit convergence. The distribution of the ratio of signal likelihood to total likelihood for all events entering the fit is also presented in Fig. 1, showing good agreement between the data and the model.

For the CP -violation parameters, we obtain

$$S = -1.62_{-0.51}^{+0.56} \pm 0.09 \pm 0.04,$$

$$C = 0.27 \pm 0.36 \pm 0.10 \pm 0.07.$$

The time-dependent distributions and asymmetry $A_{B^0/\bar{B}^0} = (N_{B^0} - N_{\bar{B}^0}) / (N_{B^0} + N_{\bar{B}^0})$ in the tagged events are represented in Fig. 2. The model-dependent mass and width of the f_0 are found to be

$$m_{f_0} = (980.6 \pm 4.1 \pm 0.5 \pm 4.0) \text{ MeV}/c^2,$$

$$\Gamma_{f_0} = (43_{-9}^{+12} \pm 3 \pm 9) \text{ MeV}/c^2.$$

These results are in agreement with previous mass and width measurements [4,14].

In summary, we have presented the first observation of $B^0 \rightarrow f_0(980)K_S^0$ and measurements of the branching fraction, resonance parameters, and CP -violating asymmetries in $B^0 \rightarrow f_0(980)(\rightarrow \pi^+ \pi^-)K_S^0$ decays. As determined from a large number of simulated experiments, our results for S and C are consistent with the standard model within 1.7 and 0.8 standard deviations, respectively. The result for S is 1.2 standard deviations from the physical limit, and the hypothesis of no mixing-induced CP violation is excluded within 2.7 standard deviations.

We are grateful for the excellent luminosity and machine conditions provided by our PEP-II colleagues, and for the substantial dedicated effort from the computing organizations that support *BABAR*. The collaborating institutions wish to thank SLAC for its support and kind hospitality. This work is supported by DOE and NSF (U.S.A.), NSERC (Canada), IHEP (China), CEA and CNRS-IN2P3 (France), BMBF and DFG (Germany), INFN (Italy), FOM (The Netherlands), NFR (Norway), MIST (Russia), and PPARC (United Kingdom). Individuals have received support from CONACyT (Mexico), A. P. Sloan Foundation, Research Corporation, and Alexander von Humboldt Foundation.

*Now at Department of Physics, University of Warwick, Coventry, United Kingdom.

†Also with Università della Basilicata, Potenza, Italy.

‡Also with IFIC, Instituto de Física Corpuscular, CSIC-Universidad de Valencia, Valencia, Spain.

§Deceased.

- [1] N. Cabibbo, Phys. Rev. Lett. **10**, 531 (1963); M. Kobayashi and T. Maskawa, Prog. Theor. Phys. **49**, 652 (1973).
- [2] Y. Grossman and M.P. Worah, Phys. Lett. B **395**, 241 (1997); M. Ciuchini *et al.*, Phys. Rev. Lett. **79**, 978 (1997); D. London and A. Soni, Phys. Lett. B **407**, 61 (1997).
- [3] A.B. Carter and A.I. Sanda, Phys. Rev. D **23**, 1567 (1981); I.I. Bigi and A.I. Sanda, Nucl. Phys. B **193**, 85 (1981); Y. Grossman and M.P. Worah, Phys. Lett. B **395**, 241 (1997); R. Fleischer, Int. J. Mod. Phys. A **12**, 2459 (1997); D. London and A. Soni, Phys. Lett. B **407**, 61 (1997).
- [4] Particle Data Group Collaboration, S. Eidelman *et al.*, Phys. Lett. B **592**, 1 (2004).
- [5] *BABAR* Collaboration, B. Aubert *et al.*, Phys. Rev. Lett. **93**, 071801 (2004); *BABAR* Collaboration, B. Aubert *et al.*, Phys. Rev. Lett. **93**, 181805 (2004); *BABAR* Collaboration, B. Aubert *et al.*, Phys. Rev. Lett. **91**, 161801 (2003).
- [6] Belle Collaboration, K. Abe *et al.*, Phys. Rev. Lett. **91**, 261602 (2003).
- [7] Throughout the paper f_0 refers to the $f_0(980)$ and its decay to $\pi^+ \pi^-$. In addition, charge conjugate decay modes are assumed unless explicitly stated.

- [8] *BABAR* Collaboration, B. Aubert *et al.*, Nucl. Instrum. Methods Phys. Res., Sect. A **479** 1 (2002).
- [9] *BABAR* Collaboration, B. Aubert *et al.*, hep-ex/0408073.
- [10] *BABAR* Collaboration, B. Aubert *et al.*, hep-ex/0408079.
- [11] *BABAR* Collaboration, B. Aubert *et al.*, Phys. Rev. Lett. **89**, 281802 (2002).
- [12] *BABAR* Collaboration, B. Aubert *et al.*, Phys. Rev. **D66**, 032003 (2002).
- [13] O. Long, M. Baak, R.N. Cahn, and D. Kirkby, Phys. Rev. D **68**, 034010 (2003).
- [14] E791 Collaboration, E.M. Aitala *et al.*, Phys. Rev. Lett. **86**, 765 (2001).